ACI MATERIALS JOURNAL TECHNICAL PAPER

Title no. 98-M45

Fracture Energy of High-Strength Concrete

by David Darwin, Shawn Barham, Rozalija Kozul, and Shuguang Luan

*The effects of water-cementitious materials ratio, age, and aggregate type on the compressive strength, flexural strength, and fracture energy of concretes with compressive strengths ranging from 20 to 99 MPa (2900 to 14,400 psi) are studied. Concrete mixtures contain either basalt or crushed limestone aggregate with maximum sizes of 12 or 19 mm (1/2 or 3/4 in.). Mixtures are tested at ages ranging from 5 to 180 days and have water-cementitious (*w/cm*) ratios ranging from 0.24 to 0.50. High-strength concrete containing the higher-strength, basalt coarse aggregate attains higher compressive and flexural strengths than high-strength concrete containing limestone. The compressive and flexural strengths of medium and normal-strength concretes (f_c' up to approximately 60 MPa [9000 psi]) are affected little by aggregate type. Concrete containing basalt yields significantly higher fracture energy than concrete containing limestone, with fracture energy governed principally by aggregate properties, independent of compressive strength, w/cm ratio, and age. Overall, as compressive strength increases, the energy stored in the material at the peak tensile load increases while the ability of the material to dissipate energy remains approximately constant. The result is increasingly brittle behavior as compressive strength increases.*

Keywords: aggregates; compressive strength; flexural strength; fracture mechanics; high-strength concrete; water-cementitious materials ratio.

INTRODUCTION

When concrete fails in tension, its behavior is characterized by both the peak stress and the energy required to fully open a crack. Fracture energy G_f is the energy required to form a crack of unit area. While the peak stress establishes the tensile strength of the material, the fracture energy controls the ease with which a crack will propagate. Recent research (Tholen and Darwin 1996; Collins and Kuchma 1999; Zuo and Darwin 2000) indicates that fracture energy plays an increasingly important role in the behavior of reinforced concrete members when tension is resisted by concrete alone. Tests show that both the bond strength between reinforcing steel and concrete and the shear strength of concrete increases more slowly than $\sqrt{f_c'}$ when $f_c' > 50$ MPa (7000 psi), even though the tensile strength of the concrete increases at least as rapidly as $\sqrt{f_c'}$ (Ahmad and Shah 1985). In particular, Zuo and Darwin (2000) demonstrated that the splice strength of reinforcing bars not confined by transverse reinforcement increases with $f_c'^{0.25}$ for 29 MPa (4250 psi) $\le f_c' \le$ 108 MPa (15,650 psi). In shear tests of full-scale reinforced concrete beams without transverse reinforcement, Collins and Kuchma (1999) observed that there was no increase in shear strength for $f_c' > 50$ MPa (7250 psi), and, in fact, there was an 18% decrease in shear strength between $f_c' = 36$ MPa (5700 psi) and 99 MPa (14,400 psi). The reason for the relatively poor performance of high-strength concrete in bond and shear is that these structural properties involve crack propagation and are thus not controlled by tensile strength alone.

The goal of this research is to investigate the relationships between compressive strength, flexural strength, fracture energy, water-cementitious materials ratio (*w/cm*), age, and aggregate type. The compressive and tensile strengths of concrete increase with decreasing *w/cm* and increasing age. For normal weight aggregates, properties have relatively little effect on the strength of normal-strength concretes, but play an increasingly important role as the compressive and tensile strengths increase. The relationship of fracture energy to these properties is less clear, with most studies showing a relative insensitivity to *w/cm* and age, and a greater sensitivity to aggregate type than is observed for compressive and tensile strength. Full details of the study are presented by Kozul and Darwin (1997) and Barham and Darwin (1999).

RESEARCH SIGNIFICANCE

This study is significant because it provides an explanation for the relatively poor structural performance of high-strength reinforced concrete members under load regimes in which the tensile properties of concrete play an important role. Recent studies (Collins and Kuchma 1999; Zuo and Darwin 2000) have demonstrated that high-strength concretes provide significantly lower bond and shear strengths than would be expected based on relationships developed for concretes with $f_c' < 50$ MPa (7000 psi).

EXPERIMENTAL WORK

Concrete specimens were tested to determine the relationships between compressive strength, flexural strength, and fracture energy as a functions of *w/cm*, age, and aggregate type. The tests were carried out in two series. Series I (Kozul and Darwin 1997) was part of a larger study to determine the effect of concrete compressive strength and reinforcing bar properties on the bond strength between reinforcing steel and concrete (Darwin et al. 1996a, 1996b; Zuo and Darwin 2000). Series I included aggregate sizes of 12 and 19 mm (1/2 and 3/4 in.) and *w/cm* ratios of 0.24 to 0.50. Tests were carried out at ages that were representative of those used for the bond test specimens, five days for normal-strength concrete and 94 to 164 days for high-strength concrete. Series II (Barham and Darwin 1999) tests used 19 mm (3/4 in.) aggregate and three concrete strength categories (normal, medium, and high) obtained using *w/cm* ratios ranging from 0.25 to 0.46. In Series II, the specimens were tested at ages of 7, 28, 56, 90, and 180 days. Crushed basalt and limestone coarse aggregates were used in both series.

Materials

Type I portland cement was used in all mixtures. Medium-strength concrete also contained Class C fly ash, while

ACI Materials Journal, V. 98, No. 5, September-October 2001.
MS No. 01-063 received February 26, 2001, and reviewed under Institute publication policies. Pertinent discussion will be published in the July-August 2002 *ACI Materials Journal* if received by April 1, 2002.

David Darwin, *FACI, is the Deane E. Ackers Professor of Civil Engineering and Director of the Structural Engineering and Materials Laboratory at the University of Kansas, Lawrence, Kans. He is a past member of the Board of Direction and the Technical Activities Committee and is past-president of the Kansas Chapter of ACI. Darwin is also past-chairman of the Publications Committee and the Concrete Research Council, and a member and past-chairman of ACI Committee 224, Cracking. He chairs the TAC Technology Transfer Committee and ACI Committee 408, Bond and Development of Reinforcement, and serves on ACI Committee 446, Fracture Mechanics; ACI-ASCE Committees 445, Shear and Torsion; and 447, Finite Element Analysis of Reinforced Concrete Structures. He is a recipient of the Arthur R. Anderson and ACI Structural Research Awards.*

Shawn Barham *is a structural engineer with Burns & McDonnell International in Kansas City, Mo. He received his BS and MS in civil engineering from the University of Kansas.*

Rozalija Kozul *is a project engineer with the Penta Building Group in Las Vegas, Nev. She received her BS and MS in civil engineering from the University of Kansas.*

Shuguang Luan *is an associate professor of civil engineering at the Dalian Fishery College, Peoples Republic of China, and was a visiting scholar at the University of Kansas from 1997 to 1998.*

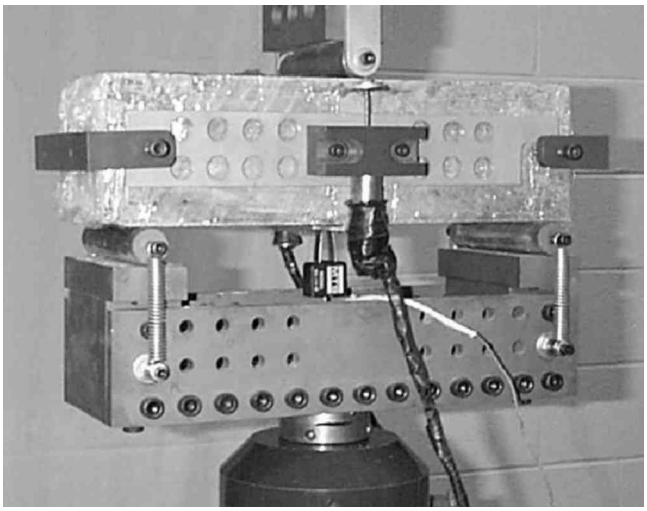

Fig. 1—Fracture energy test apparatus using closed-loop servohydraulic testing system.

high-strength concrete contained fly ash and compacted silica fume. The basalt coarse aggregate had a bulk specific gravity (ssd) of 2.64, an absorption (dry) of 0.4%, a compressive strength (measured on a 25 mm square x 75 mm [1 in. square x 3 in.] prism) of 340 MPa (50,000 psi), and a modulus of elasticity of 69 GPa (10,000,000 psi). The limestone in Series I had a bulk specific gravity (ssd) of 2.58, an absorption (dry) of 2.7%, a compressive strength of 100 MPa (15,000 psi), and a modulus of elasticity of 35 GPa (5,000,000 psi). The limestone in Series II had a bulk specific gravity (ssd) of 2.54 and an absorption (dry) of 3.9%; the limestone in Series II was not tested for strength. The fine aggregate used in the study was river sand with a bulk specific gravity (ssd) of 2.61, an absorption (dry) of 0.5%, and a fineness modulus of 2.60. A Type A normal-range water reducer and a Type F high-range water-reducing admixture were used. Mixture proportions are summarized in Table 1.

Specimens

Concrete was batched in a counter-current pan mixer. 100 x 100 x 350 mm (4 x 4 x 14 in.) prismatic specimens were used for all tests. Forms were filled with the long dimension in the vertical direction. The concrete was consolidated in three equal layers, rodded 25 times each with a 16 mm (5/8 in.) tamping rod. After rodding each layer, the forms were struck smartly 10 to 15 times with a rubber mallet. Following consolidation, the forms were sealed and stored in a horizontal position at 20 to 24 C (68 to 76 F) for 48 h. The molds were then removed and the specimens placed in lime-saturated water at 21 to 24 C (70 to 76 F). At least 24 h before the compressive specimens were tested, 25 mm (1 in.) was removed form each end using a high-speed masonry saw to achieve a 3:1 length-width ratio and capped with 1.6 mm (1/16 in.) layer of sulfur capping compound. The fracture energy specimens were prepared by cutting a 25 mm (1 in.) deep by 3 mm (1/8 in.) wide notch on one side at the midpoint perpendicular to the long direction. The specimens were then placed back in the lime-saturated water until the time of test. Specimens were covered with plastic wrap after removal from the water to minimize moisture loss during the test.

Testing

The compression tests were performed in accordance with ASTM C 39 (1996) using an 1800 kN (400 kip) capacity hydraulic testing machine at a loading rate of 0.14 to 0.34 MPa/s (20 to 50 psi/s) until failure. The 3:1 height-width ratio placed the center region of the specimen in uniaxial compression.

The flexure specimens were loaded at an extreme fiber stress rate between 0.86 and 1.21 MPa/min (125 to 175 psi/min) in accordance with ASTM C 293 (1994), using centerpoint loading in a 1800 kN (400 kip) machine for Series I and a 150 kN (35 kip) closed-loop servohydraulic testing system for Series II.

The fracture energy test followed the guidelines established by RILEM (1985) using a closed-loop testing machine under crack mouth opening displacement (CMOD) control (Fig. 1). Prior to the test, small regions on the bottom surface of the concrete on either side of the notch were dried using a hair dryer on low heat. Two steel plates with lips to fit into the sawed notch were attached on both sides of the notch using a rapid-drying glue. The clip gage used to measure the CMOD was then placed between knife edges attached to the steel plates. Two steel nails were then glued on both sides near the top of the specimen at midspan to hold the cores of two linear variable differential transformers (LVDTs) used to measured deflection. The cores were supported by washers suspended by the nails. The core housings of the LVDTs were held by aluminum bars screwed to the concrete at the mid-depth of the beam over the supports. Deflection was measured in this way so as not to include the effects of local specimen deformations at the support and load points. A data acquisition system was used to record load, CMOD, and deflection. A constant CMOD rate of 0.08 mm/min (0.003 in./min) was set so that the peak load would be attained in approximately 30 s. Tests lasted between 15 and 50 min, depending on aggregate type, specimen age, and *w/cm*.

RESULTS AND EVALUATION

The test results and comparisons of the compression, flexure, and fracture energy tests are presented. Where appropriate, the results for Series I and Series II are combined. Because of the matching ages at the time of test, most comparisons are illustrated using the results from Series II. Test results are summarized in Tables 2(a) and (b) for Series I and II, respectively.

Table 1—Concrete mixture proportions (m^3 batch), slump, and test age

Concrete type*	Batches†	*w/cm*‡	Water, kg	Cement, kg	Fly ash, kg	Silica fume, kg	Fine aggregate (SSD), kg	Coarse aggregate (SSD), kg	Type A admixture, L	Type F admixture, L	Slump, mm	Test age, days
Series I												
NB	19h	0.50	164	327	—	—	775	1105	—	—	100	5
	12h	0.50	164	327	—	—	773	1105	—	—	80	5
	12l	0.50	164	327	—	—	885	994	0.8	—	80	5
NL	12h	0.50	164	327	—	—	765	1090	0.7	—	100	5
	12l	0.50	164	327	—	—	888	973	1.0	—	100	5
HB	19h.1	0.26	116	411	24	49	714	1105	2.1	13.2	230	137
	19h.2	0.26	116	411	24	49	714	1098	2.1	11.0	240	116
	12h.1	0.24	107	412	24	49	743	1102	2.1	14.4	230	164
	12h.2	0.26	105	410	24	48	739	1096	2.1	24.2	240	149
	12h.3	0.28	116	412	24	49	714	1101	2.1	26.6	230	119
	12l.1	0.28	105	407	24	48	846	986	2.1	36.6	230	160
	12l.2	0.27	116	413	24	49	824	985	2.1	21.1	240	117
HL	12h.1	0.26	116	410	24	48	716	1074	2.4	10.5	240	148
	12h.2	0.26	117	411	24	49	721	1071	2.4	11.6	240	111
	12l	0.27	117	413	24	49	829	964	2.4	19.9	220	94
Series II												
NB	1, 2, 1-2, 3	0.46	164	356	—	—	790	1054	—	—	80, 100, -, 70	7 to 180§
NL	1, 2	0.46	164	356	—	—	813	991	—	—	110, 110	7 to 180§
MB	1, 2	0.351	148	360	63	—	764	1054	0.4	—	110, 120	7 to 180§
ML	1, 2	0.35	148	360	63	—	787	991	—	—	130, 100	7 to 180§
HB	1, 2, 3	0.266, 0.280, 0.261	133	470	28	55	683	1054	1.6	18.1, 29.6, 14.8	170, 160, 170	7 to 180§
HL	1, 2	0.250, 0.254	133	470	28	55	707	991	1.6	5.8, 9.1	180, 240	7 to 180§

*N = normal-strength concrete; M = medium-strength concrete; H = high-strength concrete; B = basalt aggregate; and L = limestone aggregate.
†12, 19 = 12, 19 mm maximum size aggregate; h, l = high, low coarse aggregate content.
‡*w/cm* = water-cementitious materials ratio; includes water in admixtures.
§Test ages = 7, 28, 56, 90, and 180 days.

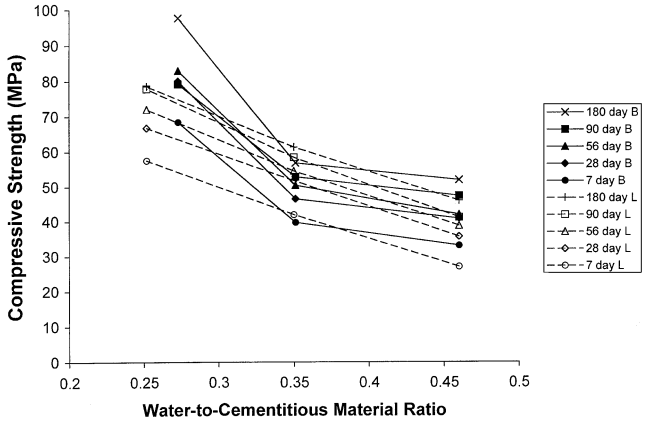

Fig. 2—Average compressive strength versus average w/cm *for concretes in Series II (B = basalt; L = limestone) (1 MPa = 145 psi).*

Compressive strength

Compressive strength f_c' is plotted versus *w/cm* and age for the Series II specimens in Fig. 2. The figure shows that basalt and limestone produce similar compressive strengths for both the normal and the medium-strength concretes. The basalt, however, produces significantly greater strengths than the limestone (with the exception of the tests at 90 days) for high-strength concrete. The greatest difference is observed at 180 days, where the basalt high-strength specimens average 25% higher compressive strengths than those containing limestone. These observations match those of other researchers (Kaplan 1959; Giaccio et al. 1992; Ozturan and Cecen 1997) who found that higher-strength aggregates have a progressively beneficial effect as compressive strength increases. The reason is that the cement paste matrix is denser and stiffer in high-strength concrete, resulting in greater compatibility in strength and stiffness between the cement paste and the aggregate, thus leading to lower stress concentrations at the matrix-aggregate interface. The tensile strength of the aggregate, rather than the interfacial strength (as in normal-strength concrete), becomes the weak link. Because of this, the compressive strength of high-strength concrete can be limited by aggregate strength. For the medium and normal-strength concretes, the two aggregates result in similar strengths, with limestone actually producing higher compressive strengths in the medium-strength concrete (Fig. 2 and Table 2[b]).

The appearance of the failure surfaces of the specimens depends on the aggregate type. In normal-strength concrete with both types of aggregate, the fracture surface was torturous, with significant crack branching. The basalt concrete had virtually no fractures through the coarse aggregate, while the limestone concrete showed evidence of some

Table 2(a)—Concrete properties for Series I

Group	Age, days	Compressive strength, MPa			Flexural strength, MPa			Fracture energy, N/m		
		Specimen 1	Specimen 2	Specimen 3	Specimen 1	Specimen 2	Specimen 3	Specimen 1	Specimen 2	Specimen 3
NB-19h	5	29.6	29.4	31.4	5.6	5.7	6.1	230	220	227
NB-12h	5	27.6	27.6	28.3	5.4	5.7	5.6	198	164	193
NB-12l	5	24.1	26.9	25.0	5.8	4.8	4.8	182	184	182
NL-12h	5	30.3	30.5	30.7	5.7	5.4	5.5	70	67	60
NL-12l	5	29.7	29.2	28.8	5.7	5.7	5.7	53	48	66
HB-19h.1	137	82.7	81.5	78.3	10.3	12.1	—	136	137	187
HB-19h.2	116	79.5	76.7	76.9	10.2	9.3	10.1	215	140	152
HB-12h.1	164	92.6	93.0	103.4	13.0	12.6	13.0	148	164	151
HB-12h.2	149	81.9	84.5	79.1	11.1	10.1	11.4	169	194	151
HB-12h.3	119	80.6	80.8	78.9	10.1	10.5	10.0	173	206	155
HB-12l.1	160	93.1	94.3	—	10.9	11.5	—	167	—	—
HB-12l.2	117	60.4	66.1	61.2	9.0	8.8	9.2	158	203	127
HL-12h.1	148	80.2	82.3	76.4	8.4	8.9	8.9	—	—	—
HL-12h.2	111	74.2	67.2	71.4	7.9	8.3	8.1	69	63	59
HL-12l	94	71.6	71.2	68.8	8.1	9.0	8.5	68	69	59

Table 2(b)—Concrete properties for Series II

Group	Compressive strength, MPa					Flexural strength, MPa					Fracture energy, N/m				
	7 days	28 days	56 days	90 days	180 days	7 days	28 days	56 days	90 days	180 days	7 days	28 days	56 days	90 days	180 days
NB1	33.8	38.0	42.3	44.3	49.7	4.8	6.4	5.7	6.0	5.7	100	106	133	133	136
NB2	30.1	41.9	39.0	46.9	50.8	4.6	6.3	5.8	5.5	5.3	143	127	140	202	133
NB1-2	35.7	42.7	44.9	51.0	55.2	5.2	6.7	5.6	5.7	5.8	131	106	131	161	138
NB3	35.4	42.8	—	—	—	5.7	6.4	—	—	—	131, 110	106, 128, 120	—	—	—
NL1	20.1	26.0	30.5	33.4	39.9	3.8	4.6	4.5	6.1	6.7	44	42	52	45	49
NL2	34.0	45.4	47.2	49.0	52.1	5.7	6.0	6.5	7.0	7.5	42	45	44	48	48
MB1	40.0	50.4	51.6	52.9	55.4	6.2	7.3	7.3	7.1	6.9	146	141	118	162	160
MB2	39.6	42.6	49.1	52.8	58.1	5.7	7.2	7.0	6.7	6.7	139	112	145	167	117
ML1	38.8	47.0	50.2	53.3	56.0	5.7	6.3	6.3	6.4	6.6	45	45	56	61	63
ML2	45.1	56.5	58.9	63.5	66.6	6.4	7.1	7.3	7.3	7.5	55	63	57	66	65
HB1	71.5	78.2	87.2	76.5	96.6	8.9	11.7	11.9	12.1	12.6	116	106	127	119	117
HB2	65.3	81.9	78.6	81.7	98.7	10.2	11.2	10.7	12.2	13.5	132	104	140	113	128
HB3	65.6	85.4	—	—	—	8.3	10.9	—	—	—	127, 137	103, 109, 142	—	—	—
HL1	51.2	66.6	67.5	70.9	71.3	5.7	7.1	7.3	7.5	7.6	28	50	39	40	45
HL2	63.7	66.9	76.5	84.7	85.7	6.9	7.6	7.7	7.7	7.8	43	42	43	41	36

transgranular fracture. In high-strength concrete, the branching was similar, but less severe than in normal-strength concrete. There was, however, a large increase in the fracture of coarse aggregate particles. In the basalt concrete, most, but not all, of the coarse aggregate fractured. The limestone concrete had complete transgranular fracture, leaving the crack surface less torturous than in the basalt concrete and the smoothest overall. The medium-strength concrete had fracture surfaces that were a composite of those observed in normal and high-strength concrete.

Flexural strength

Flexural strength is plotted versus *w/cm* and age in Fig. 3. As with compressive strength (Fig. 2), the basalt coarse aggregate provided significantly higher values for the modulus of rupture *R* than the limestone for the high-strength concrete (61% greater at 7 days and 92% greater at 180 days), but similar values for the medium and normal-strength concretes. The fracture surfaces in the flexural specimens were similar to those observed in the compression tests, although there was slightly more transgranular fracture in the flexural specimens. Flexural strength increased with age more slowly than compressive strength.

Fracture energy

Fracture energy is the energy dissipated per unit area during the formation of a crack. The energy is dissipated within the fracture process zone, the region in front of a crack tip where the stress decreases as the crack opens. The area of fracture is the projected area on a plane perpendicular to the direction of stress. A schematic is presented in Fig. 4.

In the current study, fracture energy is determined using a notched beam in three-point bending. The average deflection is measured at the centerline of the beam. Load-deflection curves are plotted, with the energy W_0 representing the area under the curve.

RILEM (1985) and Hillerborg (1985) suggest that fracture energy be calculated using the following expression

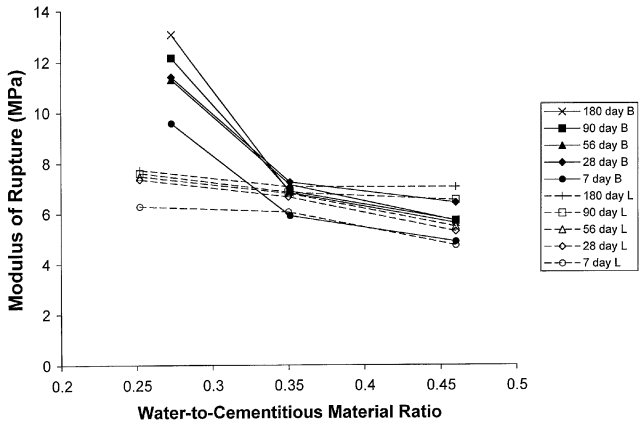

Fig. 3—Average modulus of rupture versus average w/cm *for concretes in Series II (B = basalt; L = limestone) (1 MPa = 145 psi).*

$$G_f = (W_0 + mg\delta_f)/A \quad (1)$$

where G_f = fracture energy (N-m or lb-in.); W_0 = area under the load-deflection curve (N-m or lb-in.); $m = m_1 + 2m_2$ (kg or slug); m_1 = mass of the beam between the supports; m_2 = mass of the loading frame not attached to the load machine that follows the specimen until failure; g = acceleration due to gravity; δ_f = final deflection of the beam (m or in.); and A = cross-sectional area of the beam above the notch (m^2 or $in.^2$).

The need for the term $mg\delta_f$ results from the fact that the imposed load from the machine is not the only load acting on the specimen during the test; the weight of the specimen between the supports and the weight of the testing equipment supported by the specimen also play a role. Therefore, the measured load-deflection curve does not account for the full load on the beam and thus does not reflect the total energy necessary to cause fracture.

A hypothetically complete load-deflection curve is shown in Fig. 4. P_1 is the additional load caused by the weight of the specimen $0.5m_1g$ and the weight of loading equipment m_2g.

The total energy required to fully fracture the specimen is

$$W = W_0 + W_1 + W_2 \quad (2)$$

where $W_1 = P_1\delta_f = (0.5m_1 + m_2)g\delta_f = 0.5mg\delta_f$.

Hillerborg (1985) demonstrated that W_2 is approximately equal to W_1, making the total energy

$$W = W_0 + 2P_1\delta_f = W_0 + mg\delta_f \quad (3)$$

This total is divided by the projected area of fracture A to give the fracture energy G_f.

Figure 5 compares the load-deflection curves from fracture tests of normal-strength concretes containing basalt and limestone coarse aggregates in Series I. The area under the curve for the concrete containing basalt is significantly greater than that for the concrete containing limestone. The concretes exhibit nearly identical peak loads, but the concrete containing basalt is able to sustain a maximum deflection that is nearly three times greater. The difference in the areas under the curves translates into a significantly higher fracture energy for the basalt concrete than for the limestone

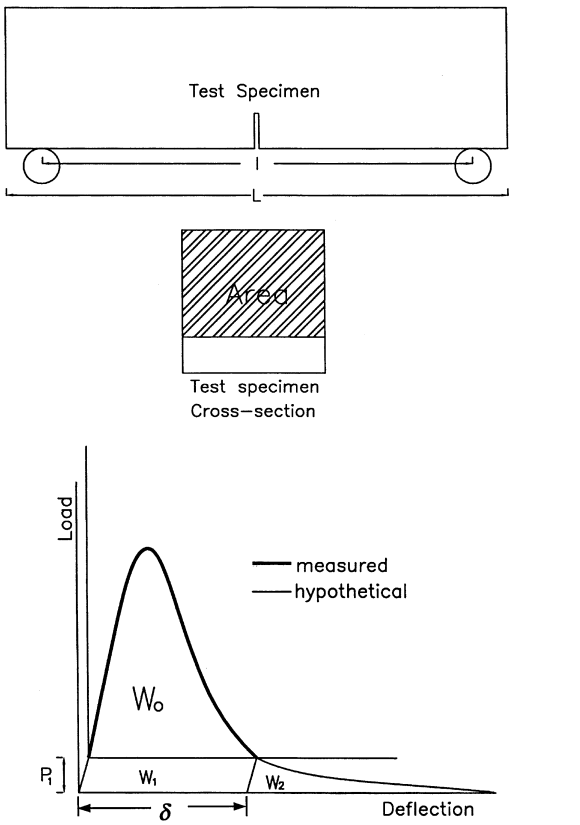

Fig. 4—Schematic of fracture energy test specimen (depth = width = 100 mm [4 in.]; notch depth = 25 mm [1 in.]; L = 350 mm [14 in.]; l = 300 mm [12 in.]); and load-deflection curve.

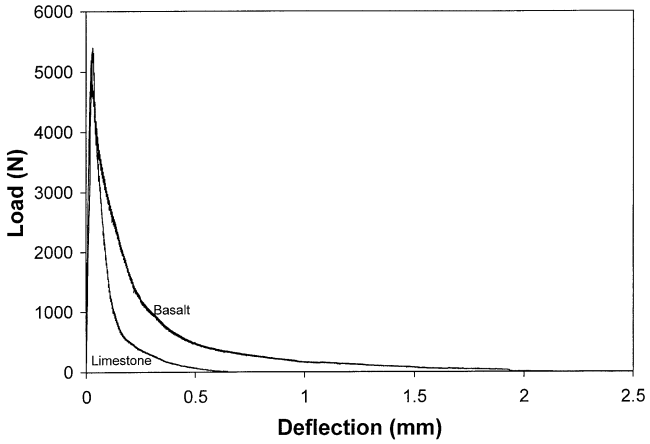

Fig. 5—Load-deflection curves for fracture specimens containing 12 mm (1/2 in.) basalt and limestone normal-strength concretes (NB-12h and NL-12h) (1 N = 0.225 lb, 1 mm = 0.0394 in.).

concrete: 193 N/m (1.10 lb/in.) versus 70 N/m (0.40 lb/in.). As will be demonstrated, G_f is principally a function of coarse aggregate properties and is largely independent of age and *w/cm.*

Figure 6 compares the load-deflection curves from fracture tests of high and normal-strength specimens containing basalt in Series I. The high-strength concrete specimen exhibits a significantly higher peak load (9 versus 5.6 kN), while the normal-strength specimen exhibits more ductile behavior on the descending branch of the curve and a greater

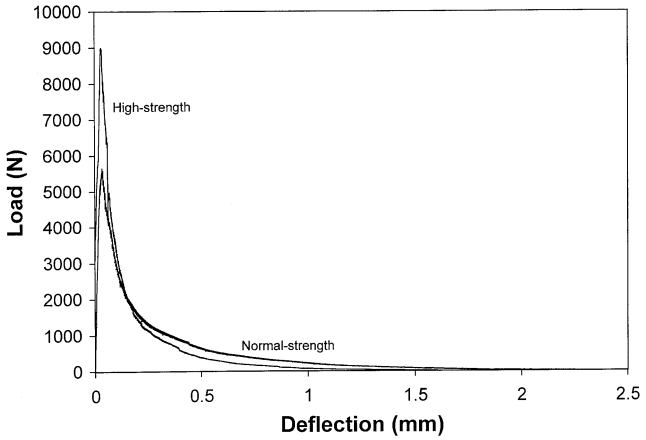

Fig. 6—Load-deflection curves for fracture specimens fabricated with normal and high-strength concretes containing 12 mm (1/2 in.) basalt coarse aggregate (HB-12l.2 and NB-12l) (1 N = 0.225 lb, 1 mm = 0.0394 in.).

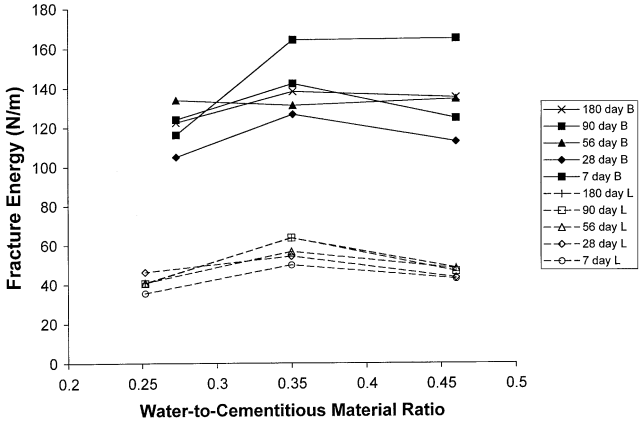

Fig. 7—Average fracture energy versus average w/cm *for concretes in Series II (B = basalt; L = limestone) (1 N/m = 5.7 ´ 10^{-3} lb/in.).*

maximum deflection. Overall, the areas under the two curves are similar, with G_f actually higher for the normal-strength concrete than for high-strength concrete: 182 versus 158 N/m (1.05 versus 0.90 lb/in.).

The observations obtained for specific specimens in Fig. 5 and 6 can be generalized, as demonstrated in Fig. 7, in which fracture energy is compared with the *w/cm* and age for the specimens in Series II. The figure shows that the fracture energy of the concretes containing basalt is consistently more than two times greater than the fracture energy of the concretes containing limestone. It also demonstrates that fracture energy is nearly constant as a function of *w/cm* and age (in this case, for ages of 7 to 180 days). In fact, on the average, the concretes with the lowest *w/cm* ratios exhibit the lowest values of G_f. Similar results are obtained for Series I (Table 2[a]).

The failure surfaces in the fracture tests were similar to those in the compression and flexure tests. The high-strength concrete specimens containing limestone had the smoothest surfaces, while the normal-strength specimens containing basalt had the roughest.

Comparisons of properties

Flexural strength versus compressive strength—The relationship between flexural strength (modulus of rupture R) and compressive strength has been well researched. ACI Committee 363 (1992) developed the following expression to describe this relationship for 21 MPa (3000 psi) ≤ f_c' ≤ 83 MPa (12,000 psi).

$$R = 0.94 f_c'^{0.5} \text{ (MPa)} \quad (4a)$$

$$R = 11.7 f_c'^{0.5} \text{ (psi)} \quad (4b)$$

The results of this study are plotted, along with Eq. (4), in Fig. 8. (Note: Eq. [4] is based on compressive specimens with height-width ratios of 2:1, which typically yield slightly higher strengths than the 3:1 ratio specimens used in this study, and on flexural strengths for specimens under third-point loading, which give slightly lower strengths than the center-point loading used in this study.) The modulus of rupture R increases almost linearly with compressive strength for the concrete containing basalt coarse aggregate, while the

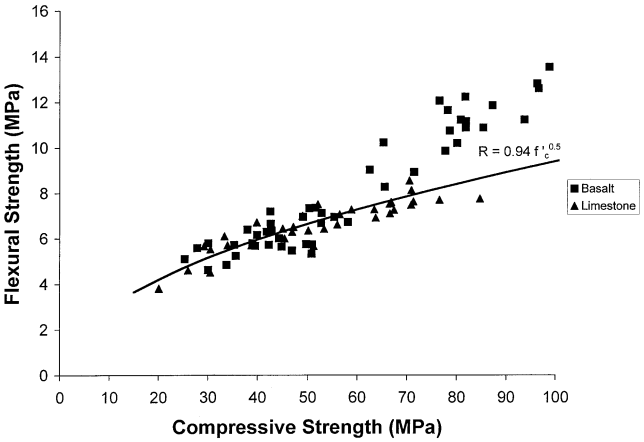

Fig. 8—Flexural strength (modulus of rupture) versus compressive strength for concretes in Series I and II (curve developed by ACI Committee 363 [1992]) (1 MPa = 145 psi).

data points for the limestone concrete follow Eq. (4). As discussed previously, the two coarse aggregates yield similar flexural strengths for the normal and medium-strength concretes, while the basalt yields significantly higher flexural strength than limestone for high-strength concrete.

Fracture energy versus compressive strength—Figure 9 compares fracture energy with compressive strength for all specimens in the study. As suggested in Fig. 7, fracture energy shows no clear relationship to compressive strength. If there is a trend, it is, at most, a slight drop in G_f with increasing f_c'. Figure 9 shows that fracture energy depends primarily on aggregate type, with the concretes containing basalt yielding significantly higher fracture energies than the concretes containing limestone. This compares favorably with research by Jensen and Hansen (2001), who observed a dependence of fracture energy on aggregate type and independence from compressive strength for concretes with compressive strengths up to approximately 50 MPa (7000 psi). Zhong and Wu (2001) also observed the independence of compressive strength and fracture energy for concretes with cube strengths up to 114 MPa (16,500 psi). Other researchers have observed only small changes in G_f with increases in f_c'. Get-

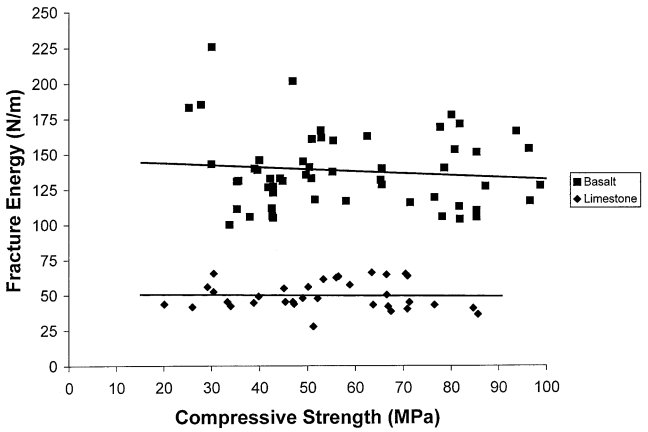

Fig. 9—Fracture energy versus compressive strength for concretes in Series I and II (1 N/m = 5.7 ´ 10^{-3} lb/in., 1 MPa = 145 psi).

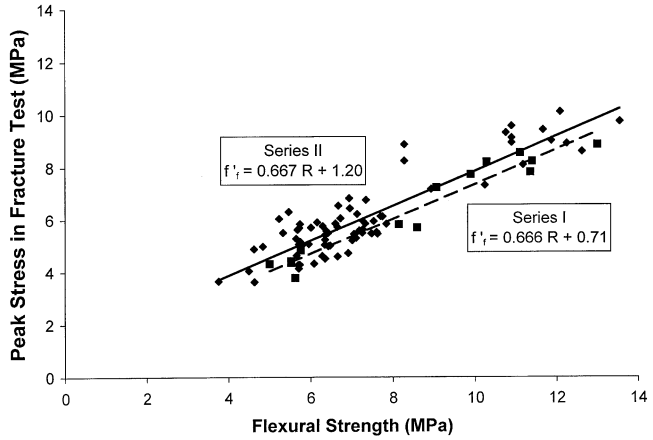

Fig. 10—Peak stress in fracture tests versus flexural strength for concretes in Series I and II (1 MPa = 145 psi).

tu, Ba ant, and Karr (1990) found that an increase in compressive strength of 160% resulted in an increase in fracture energy of only 12%. Giaccio, Rocco, and Zerbino (1993) observed that fracture energy increased as compressive strength increased, but only at a fraction of the rate. Xie, Elwi, and MacGregor (1995) found increases in compressive strength of 29 and 53% resulted in fracture energy increases of only 11 and 13%, respectively. Zhou, Barr, and Lydon (1995) found that fracture energy increased or decreased with an increase in compressive strength, depending on the aggregate.

Peak bending stresses in fracture tests versus flexural strength—The peak stresses in the fracture tests f_f' are calculated using the peak load and net section at the plane of the notch. The peak stresses in the fracture tests are compared to flexural strength *R* in Fig. 10. As shown in the figure, the two values of stress are nearly linearly related. The relationships shown in Fig. 10 are of some importance because, based on the close relationship between flexural strength and compressive strength (Fig. 8), peak fracture stress will increase with compressive strength. This observation leads directly to an explanation of the performance of high-strength concrete members in tension.

Problems with high-strength concrete

Figure 9 and 10 are useful in understanding problems related to the fracture properties of high-strength concrete. As shown in Fig. 9, high and normal-strength concretes have similar fracture energies. Since high-strength concrete has dissipated more of its fracture energy by the time it has reached the peak tensile stress, it has less energy available to slow crack propagation once the stress begins to drop (softening portion of the curve [Fig. 6]). This, coupled with the fact that high-strength concrete has a higher driving force (strain energy stored at the peak load), results in more rapid crack growth and more brittle failure than in normal-strength concrete. Thus, although the tensile strength of concrete increases along with compressive strength (at least with $\sqrt{f_c'}$), the lower capability of the higher-strength material to prevent crack propagation results in a lower rate of increase in structural capacity. These observations largely explain the relatively poor performance of high-strength concretes in structural applications in which the tensile properties of the concrete play an important role, such as bond between reinforcing steel and concrete (Zuo and Darwin 2000) and shear (Collins and Kuchma 1999).

CONCLUSIONS

The following conclusions are based on the tests and evaluations presented in this paper.

1. High-strength concrete containing high-strength aggregate, such as basalt, has higher compressive and flexural strengths than concrete with a similar *w/cm* and a weaker aggregate, such as limestone. The compressive and flexural strengths of medium and normal-strength concretes are little affected by the strength of aggregate;
2. The fracture energy of concrete is governed principally by the properties of the coarse aggregate, with higher-strength aggregates producing concretes with higher fracture energies;
3. For concretes at least five days old, fracture energy is independent of compressive strength, *w*/*cm*, and age;
4. There is a close relationship between the peak bending stresses in fracture and flexural test specimens; and
5. Overall, as the compressive strength of concrete increases, the energy stored in the material at the peak tensile load increases, while the ability of the material to dissipate energy remains approximately constant. The result is increasingly brittle behavior as compressive strength increases.

ACKNOWLEDGMENTS

This paper is based on research supported by the National Science Foundation under Research Grant No. CMS-9402563, the U.S. Department of Transportation Federal Highway Administration, and the Lester T. Sunderland Foundation. Silica fume and chemical admixtures were provided by Master Builders Technologies. Portland cement and fly ash were provided by Lawrence Ready Mix. The basalt coarse aggregate was supplied by Geiger Ready-Mix and Iron Mountain Trap Rock Co. Additional support was provided by Dayton Richmond. A summary of this research was presented in a Keynote Speech at the Fall 2000 Convention of the Korea Concrete Institute (Darwin 2000).

REFERENCES

ACI Committee 363, 1992, "State-of-the-Art Report on High-Strength Concrete (ACI 363R-92)," *ACI Manual of Concrete Practice*, 1997 Edition, Part 1, American Concrete Institute, Farmington Hills, Mich.

Ahmad, S. H. and Shah, S. P., 1985, "Standard Properties of High Strength Concrete and Its Implications for Precast Prestressed Concrete," *PCI Journal*, V. 30, No. 6, Nov.-Dec., pp. 92-119.

ASTM C 39-96, 1996, "Standard Test Method for Compressive Strength of Cylindrical Concrete Specimens," American Society for Testing and Materials, West Conshohocken, Pa., 5 pp.

ASTM C 293-94, 1994, "Standard Test Method for Flexural Strength of Concrete (Using Simple Beam with Center-Point Loading)," American Society for Testing and Materials, West Conshohocken, Pa., 3 pp.

Barham, S., and Darwin, D., 1999, "Effects of Aggregate Type, Water-to-Cementitious Material Ratio, and Age on Mechanical and Fracture Properties of Concrete," *SM Report* No. 56, University of Kansas Center for Research, Lawrence, Kans., 95 pp.

Collins, M. P., and Kuchma, D., 1999, "How Safe Are Our Large, Lightly Reinforced Concrete Beams, Slabs, and Footings?" *ACI Structural Journal*, V. 96, No. 4, July-Aug., pp. 482-490.

Darwin, D.; Tholen, M. L.; Idun, E. K.; and Zuo, J., 1996a, "Splice Strength of High Relative Rib Area Reinforcing Bars," *ACI Structural Journal*, V. 93, No. 1, Jan.-Feb., pp. 95-107.

Darwin, D.; Zuo, J.; Tholen, M. L.; and Idun, E. K., 1996b, "Development Length Criteria for Conventional and High Relative Rib Area Reinforcing Bars," *ACI Structural Journal*, V. 93, No. 3, May-June, pp. 347-359.

Darwin, D., 2000, "Fracture of High-Strength Concrete: Implications for Structural Applications," *Proceedings*, Korea Concrete Institute, V. 12, No. 2, pp. 11-30.

Gettu, R.; Ba ant, Z. P.; and Karr, M. E., 1990, "Fracture Properties and Brittleness of High-Strength Concrete," *ACI Materials Journal*, V. 87, No. 6, Nov.-Dec., pp. 608-617.

Giaccio, G.; Rocco, C.; Violini, D.; Zappitelli, J.; and Zerbino, R., 1992, "High-Strength Concretes Incorporating Different Coarse Aggregates," *ACI Materials Journal*, V. 89, No. 3, May-June, pp. 242-246.

Giaccio, G.; Rocco, C.; and Zerbino, R., 1993, "The Fracture Energy (G_F) of High-Strength Concretes," *Materials and Structures*, V. 26, No. 161, Aug.-Sept., pp. 381-386.

Hillerborg, A., 1985, "The Theoretical Basis of a Method to Determine the Fracture Energy G_f of Concrete," *Materials and Structures*, V. 18, No. 106, pp. 291-296.

Jensen, E. A., and Hansen, W., 2001, "Fracture Energy Test for Highway Concrete—Determining the Effect of Coarse Aggregate on Crack Propagation Resistance," *Transportation Research Record* 1730, pp. 10-16.

Kaplan, M. F., 1959, "Flexural and Compressive Strength of Concrete as Affected by the Properties of Coarse Aggregate," ACI JOURNAL, *Proceedings* V. 30, No. 11, Nov., pp. 1193-1208.

Kozul, R., and Darwin, D., 1997, "Effects of Aggregate Type, Size, and Content on Concrete Strength and Fracture Energy," *SM Report* No. 43, University of Kansas Center for Research, Inc., Lawrence, Kans., 85 pp.

Ozturan, T., and Cecen, C., 1997, "Effects of Coarse Aggregate Type on Mechanical Properties of Concretes with Different Strengths," *Cement and Concrete Research*, V. 27, No. 2, Jan., pp. 165-170.

RILEM, 1985, TC 50-FMC, Fracture Mechanics of Concrete, "Determination of the Fracture Energy of Mortar and Concrete by Means of Three-Point Bend Tests on Notched Beams," RILEM Recommendation, *Materials and Structures*, V. 18, No. 16, pp. 287-290.

Tholen, M. L., and Darwin, D., 1996, "Effects of Deformation Properties on the Bond of Reinforcing Bars," *SM Report* No. 42, University of Kansas Center for Research, Inc., Lawrence, Kans., 370 pp.

Xie, J.; Elwi, A. E.; and MacGregor, J. G., 1995, "Mechanical Properties of Three High-Strength Concretes Containing Silica Fume," *ACI Materials Journal*, V. 92, No. 2, Mar.-Apr., pp. 135-145.

Zhong, D., and Wu, K., 2001, "Fracture Properties of High-Strength Concrete," *Journal of Materials in Civil Engineering*, ASCE, V. 13, No. 1, Jan.-Feb., pp. 86-88.

Zhou, F. P.; Barr, B. I. G.; and Lydon, F. D., 1995, "Fracture Properties of High-Strength Concrete with Varying Silica Fume Content and Aggregates," *Cement and Concrete Research*, V. 25, No. 3, pp. 543-552.

Zuo, J., and Darwin, D., 2000, "Splice Strength of Conventional and High Relative Rib Area Bars in Normal and High Strength Concrete," *ACI Structural Journal*, V. 97, No. 4, July-Aug., pp. 630-641.